

AIRS

Improving Weather Forecasting and Providing New Data on Greenhouse Gases

BY MOUSTAFA T. CHAHINE, THOMAS S. PAGANO, HARTMUT H. AUMANN, ROBERT ATLAS,*
CHRISTOPHER BARNET, JOHN BLAISDELL, LUKE CHEN, MURTY DIVAKARLA, ERIC J. FETZER, MITCH GOLDBERG,
CATHERINE GAUTIER, STEPHANIE GRANGER, SCOTT HANNON, FREDRICK W. IRION, RAMESH KAKAR,
EUGENIA KALNAY, BJORN H. LAMBRIGTSEN, SUNG-YUNG LEE, JOHN LE MARSHALL, W. WALLACE McMILLAN,
LARRY McMILLIN, EDWARD T. OLSEN, HENRY REVERCOMB, PHILIP ROSENKRANZ, WILLIAM L. SMITH,
DAVID STAELIN, L. LARRABEE STROW, JOEL SUSSKIND, DAVID TOBIN, WALTER WOLF, AND LIHANG ZHOU

The Atmospheric Infrared Sounder (AIRS), the hyperspectral infrared sounder on the NASA *Aqua* mission, both improves operational weather prediction and provides high-quality research data for climate studies.

The Atmospheric Infrared Sounder (AIRS), and its two companion microwave instruments, the Advanced Microwave Sounding Unit (AMSU) and the Humidity Sounder for Brazil (HSB), form the integrated atmospheric sounding system flying on the Earth Observing System (EOS) *Aqua* spacecraft since its launch in May 2002.¹ The primary scientific achievement of AIRS has been to improve weather prediction (Le Marshall et al. 2005a,b,c) and to study the water and energy cycle (Tian et al. 2006). AIRS also provides information on several greenhouse gases. The measurement goal of AIRS is the retrieval of temperature and precipitable-water vapor profiles with accuracies approaching those of conventional radiosondes. In the following text we use the terms AIRS and AIRS–AMSU–HSB interchangeably.

¹ The HSB ceased functioning after 5 February 2003. This did not have an impact on the accuracy, coverage, or resolution of the AIRS core data product, but its loss has had a significant impact on AIRS research products.

A comprehensive set of articles on AIRS and AMSU design details, prelaunch calibration, and prelaunch retrieval performance expectations were published in a special issue of *IEEE Transactions on Geoscience and Remote Sensing* (2003, vol. 41, no. 2). This paper discusses the performance of AIRS and examines how it is meeting its operational and research objectives based on the experience of more than 2 yr with AIRS data. We describe the science background and the performance of AIRS in terms of the accuracy and stability of its observed spectral radiances. We examine the validation of the retrieved temperature and water vapor profiles against collocated operational radiosondes, and then we assess the impact thereof on numerical weather forecasting of the assimilation of the AIRS spectra and the retrieved temperature. We close the paper with a discussion on the retrieval of several minor tropospheric constituents from AIRS spectra.

Science objectives. The high-level measurement requirements for AIRS, defined during the mid-1980s

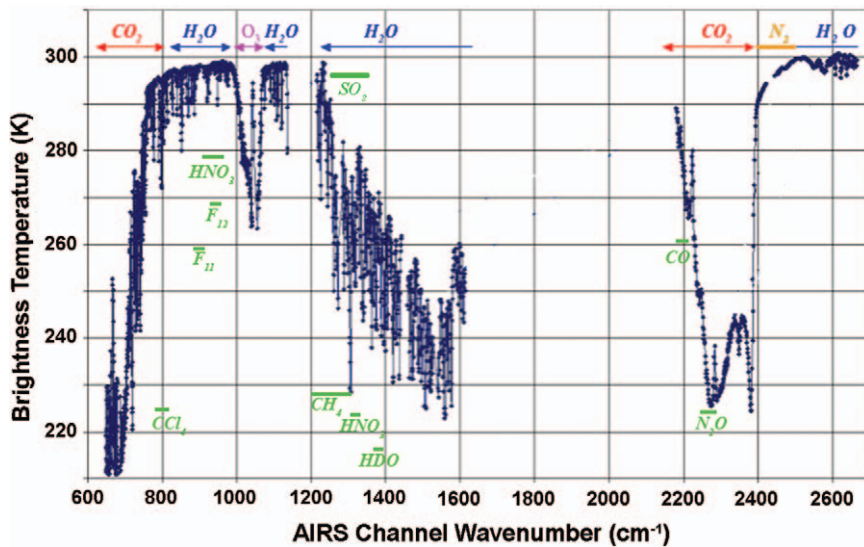


FIG. 1. The measured AIRS infrared spectrum contains a wealth of information about the atmosphere, including water vapor, temperature, and minor gases such as CO_2 , CO , CH_4 , O_3 , and SO_2 .

by the Interagency Sounder Team, were focused primarily on improving weather prediction by obtaining radiosonde-quality retrievals from satellites in polar orbit. The goal was referred to as “one degree Kelvin per kilometer,” that is, rms accuracy with 1-km vertical resolution (see Aumann et al. 2003a).

Weather and climate processes are intimately linked by water vapor, as pointed out by Chahine (1992). A recent study by the National Research Council (2004) and the Intergovernmental Panel on Climate Change (IPCC; Houghton et al. 2001) showed that the Earth’s climate can undergo changes in response to increasing concentrations of other greenhouse gases and aerosols, and that these changes may profoundly affect atmospheric water vapor, clouds, and precipitation patterns. Accurate knowledge of

the distribution of water held in the atmosphere is indispensable to predicting the amount, the time, and the location of precipitation. Accurate data, global in scope and of a much greater density than that provided by the current radiosonde network, are required to advance the development of water cycle models. AIRS data, in particular, open the possibility of investigating the impact of mesoscale dynamics on moisture in the middle and upper troposphere, which most significantly contributes to the planetary greenhouse effect.

In addition to water and temperature, AIRS data also contain information about the distribution of ozone (O_3), carbon dioxide (CO_2), carbon monoxide (CO), methane (CH_4), and other relevant forcing factors such as cloud distribution, cloud opacity, and aerosols. Converting these observations into information that is useful in studying global environment will require a broad understanding of atmospheric chemistry, radiation, and dynamics processes, as well as their combined effects on the climate system.

THE SOUNDING SYSTEM. Requirements. The AIRS–AMSU–HSB sounding system on *Aqua* is the outcome of extensive scientific and technical studies by the AIRS Team, covering instrument design, atmospheric spectroscopy, radiative transfer, scene

AFFILIATIONS: CHAHINE, PAGANO, AUMANN, CHEN, FETZER, GRANGER, IRION, LAMBRIGHTSEN, LEE, and OLSEN—Jet Propulsion Laboratory, California Institute of Technology, Pasadena, California; ATLAS and SUSSKIND—NASA Goddard Space Flight Center, Greenbelt, Maryland; BARNET, GOLDBERG, McMILLIN, and WOLF—NOAA/NESDIS, Camp Springs, Maryland; BLAISDELL—SAIC, Beltsville, Maryland; DIVAKARLA—STG, Inc., Reston, Virginia; GAUTIER—University of California, Santa Barbara, Santa Barbara, California; KAKAR—NASA Headquarters, Washington, DC; KALNAY—University of Maryland, College Park, College Park, Maryland; LE MARSHALL—Joint Center for Satellite Data Assimilation, Camp Springs, Maryland; HANNON, McMILLAN, and STROW—University of Maryland, Baltimore County, Baltimore, Maryland; REVERCOMB and TOBIN—University of Wisconsin—Madison, Madison, Wisconsin; ROSENKRANZ

and STAELIN—Massachusetts Institute of Technology, Cambridge, Massachusetts; SMITH—Hampton University, Hampton, Virginia; ZHOU—QSS Group, Lanham, Maryland

***CURRENT AFFILIATION:** NOAA Atlantic Oceanographic and Meteorological Laboratory, Miami, Florida

CORRESPONDING AUTHOR: Dr. Moustafa T. Chahine, Jet Propulsion Laboratory, California Institute of Technology, Pasadena, CA 91109

E-mail: chahine@jpl.nasa.gov

The abstract for this article can be found in this issue, following the table of contents.

DOI:10.1175/BAMS-87-7-911

In final form 3 March 2006

©2006 American Meteorological Society

coregistration, and instrument data analysis and processing. Early on, the AIRS Team recognized that the virtual omnipresence of clouds limits the accuracy and yield from infrared sounding. This limitation can be overcome by applying “cloud clearing” techniques through an analytical process combining infrared and microwave data (see the “AIRS cloud clearing” section of this paper).

The AIRS instrument views the atmospheric infrared spectrum, shown in Fig. 1, in 2,378 channels with a nominal spectral resolving power

$$\frac{\lambda}{\Delta\lambda} = 1200,$$

covering more than 95% of the Earth’s surface and returning about three million spectra daily. The design of AIRS represents a breakthrough in infrared space instrumentation, in both measurement accuracy and long-term stability.

The AIRS instrument also includes four visible and near-infrared channels and is complemented by three microwave instruments: AMSU A1 and A2 (a two-unit 15-channel temperature sounding instrument operating in the 23–90-GHz spectral range) and HSB (a single-unit four-channel water vapor sounder

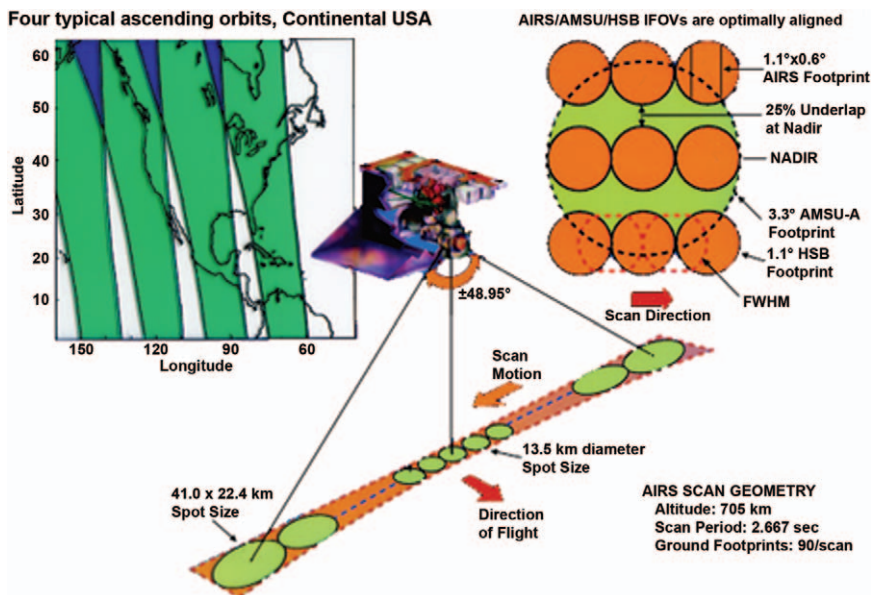


FIG. 2. AIRS scanning configuration ensures coregistration with the AMSU (upper-right corner), allowing for cloud clearing at the AMSU spatial resolution and providing global coverage of 95% of the Earth’s surface every day.

operating with three channels near 183 GHz and one channel at 150 GHz). The footprints of the microwave and infrared sounders are coregistered at the surface (see Fig. 2), a requirement for cloud clearing. A summary of the AIRS infrared observing characteristics is given in Table 1.

This integrated sounding system incorporated a number of significant advances achieved in remote sensing over the past 40 yr (see Aumann et al. 2003a). Implementation of the instrument design required new technologies, such as advanced cryocoolers, longwave infrared detectors, and integrated focal-plane signal-processing electronics. Many of these technologies were not available at the outset, but were subsequently developed by several industrial partners of the AIRS Project.

AIRS radiometric and spectral performance accuracy and stability. Key for the operational use of any sounding system is the radiometric and spectral stability of the calibrated, geolocated radiance observations known as level 1B (L1B). Excellent accuracy and stability were expected based on the repeatability of the AIRS preflight sensor calibration (Pagano et al. 2003). The accuracy of the spectral calibration at better than 1 part in 105, with a long-term stability of 1 part in 106, has been confirmed in space by comparison of the observed spectral radiances with those calculated from the

TABLE 1. Summary of AIRS characteristics.	
Spectral coverage in frequency, ν	650–2665 cm^{-1} in three bands
Number of channels	2378
Spectral sampling	$\nu/2400 \text{ cm}^{-1}$
Spectral resolution	$\nu/1200 \text{ cm}^{-1}$
NEDT at a 250-K background	0.07–0.5 K
Coverage	Global
AIRS FOVs per AMSU-A FOV	9
Instantaneous FOV	1.1°
Projected AIRS FOV size	13.5 km
Projected AMSU FOV size	45 km
AIRS data rate	1.27 Mb s^{-1}

European Centre for Medium-Range Weather Forecasts (ECMWF) analysis (Strow et al. 2006).

The radiometric accuracy and stability of AIRS radiances has been confirmed by several fundamentally different types of comparisons, including 1) the results of the daily measurements of sea surface temperature (SST), 2) direct spectral radiance comparisons from aircraft observations, and 3) low-temperature surface radiances from Antarctica. The daily measurements of the SST from AIRS measurements at 2616 cm^{-1} (Aumann et al. 2003b) are used as a test of both accuracy and stability. This specific spectral channel has the highest atmospheric transmittance in the entire IR spectrum (Chahine 1981). Attenuation of surface-emitted radiation at 2616 cm^{-1} by atmospheric gases is less than 0.4 K (expressed as brightness temperature equivalent) for a wide range of atmospheric conditions. Figure 3 shows the difference between the derived sea surface temperature from the AIRS 2616 cm^{-1} channel (sst2616) and the National Centers for Environmental Prediction (NCEP) day–night average of Real Time Global Sea Surface Temperature (RTGSST) under nighttime cloud-free conditions (Aumann et al. 2004) for the first 2 yr of the AIRS data. The surface temperature for the tropical oceans varies with seasons between 298 and 320 K. Each point in Fig. 3 represents the mean difference between the RTGSST and sst2616 for about 10^4 cloud-free spectra per day. A least-squares fit through the differences as a function of time (solid line) has a mean value of -0.57 K and no significant trend. The nominal trend is $-5 \times 10^{-3}\text{ K yr}^{-1}$, with $8 \times 10^{-3}\text{ K yr}^{-1}$ uncertainty (Aumann 2006). The sst2616 measure-

ments validate the stability of the National Institute of Standards and Technology (NIST) traceable onboard blackbody calibration source used for the calibration of all 2378 AIRS channels. Recent analysis of 3 yr of AIRS data (Aumann et al. 2006) shows the absolute accuracy of the radiance at 2616 cm^{-1} remaining at the 0.2-K level. The cold bias observed at 2616 cm^{-1} is very close to the expected bias: 0.4 K of the cold bias can be traced to the difference between the AIRS nighttime skin temperature measurements and the RTGSST day–night average of bulk-layer ($\sim 2\text{ m}$ depth) temperatures, and 0.2 K is due to residual cloud contamination of the nominally cloud-free AIRS observations.

Coincident spectral radiance observations from aircraft (Tobin et al. 2004) and from Dome Concordia in Antarctica (Walden et al. 2006), with NIST traceability and documented high absolute accuracy over a wide spectral range, have confirmed that the accuracy of the calibrated AIRS radiances is better than 0.2 K at temperatures between 240 and 300 K over the full AIRS spectral range. The continued validation of the AIRS data over a wide range of temperatures and spectral frequencies will provide the higher-quality assessment of the AIRS radiometric accuracy and stability needed to support climate applications.

AIRS CLOUD CLEARING. Less than 1% of the AIRS-observed fields are found to be cloud free at the instrument noise level. This fraction can be improved using the process called cloud clearing. The basic concept of cloud clearing is presented in the sidebar. Variant cloud-clearing approaches have been applied in the Advanced Television Infrared Observation Satellite (TIROS) Operational Vertical Sounder (TOVS) system using the High-Resolution Infrared Sounder (HIRS) and the Microwave Sounding Unit (MSU), and HIRS/2 and AMSU. The physical retrieval algorithm (PRA) (Chahine et al. 2001) forms the basis for the cloud clearing of AIRS radiances within each AMSU footprint and for the retrieval of temperature and water vapor, as described by Susskind et al. (2003).

We have compared the AIRS radiance spectra with spectra calculated using the ECMWF temperature and moisture profile from the nearest GCM grid point in space and time. The collocation mismatch can be as much as 50 km and 1.5 h (half the gridpoint spacing). The metric for the comparison is the mean and standard deviation (stddev) of observed radiance spectra (Obs) minus the radiance spectra calculated using the ECMWF profiles (Calc). We use nighttime ocean data to eliminate uncertainty in surface emis-

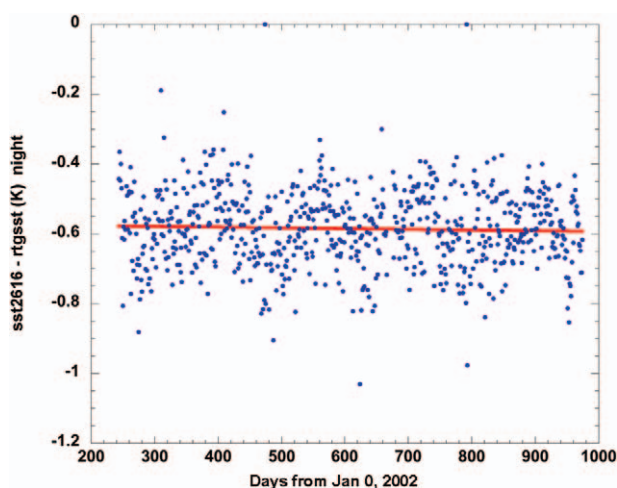


FIG. 3. The difference between the AIRS 2616 cm^{-1} derived night sea surface temperature and the NCEP GCM day–night average sea surface temperature has been stable to better than $8 \times 10^{-3}\text{ K yr}^{-1}$ since September 2002.

CLOUD CLEARING: AN INTRODUCTION

Let us consider the IR radiance $\tilde{I}(\nu)$ at frequency ν measured in the presence of clouds by an instrument such as AIRS over a given FOV. This observed radiance is composed of two major components: 1) the upwelling radiance emitted from the surface and the atmosphere below the clouds, passing through transmissive clouds and reaching the satellite, which we designate as $I(\nu)$, and 2) the radiance emitted from the clouds and the atmosphere above them.

In order to separate these two components and retrieve $I(\nu)$, which we shall call “cloud-cleared radiance” or “clear column radiance,” we start by expanding the difference between $\tilde{I}(\nu)$ and $I(\nu)$ in terms of an expansion function as

$$\tilde{I}_1(\nu) - I_1(\nu) = a_1 g(\nu, p, \varepsilon, \dots) + \dots,$$

where $g(\nu, p, \varepsilon, \dots)$ is the expansion function that need not be defined explicitly, and a is a constant independent of frequency. The above expansion can have as many terms as needed, but for simplicity we will use one term only, that is, allowing one degree of freedom. Next, we consider a second FOV adjacent to the first and write

$$\tilde{I}_2(\nu) - I_2(\nu) = a_2 g(\nu, p, \varepsilon, \dots) + \dots.$$

We ratio the above two expressions and eliminate the expansion function g to get

$$\frac{\tilde{I}_1(\nu) - I_1(\nu)}{\tilde{I}_2(\nu) - I_2(\nu)} = \frac{a_1}{a_2}.$$

We assume the difference in the observed radiance is due largely to cloud amount, while all other surface and atmospheric parameters remain the same for the two FOVs that is, $I_1(\nu) = I_2(\nu)$. By dropping the subscripts and rearranging the terms, we obtain the expression for the cloud-cleared radiance as

$$I(\nu) = \tilde{I}(\nu) + \eta[\tilde{I}_1(\nu) - \tilde{I}_2(\nu)],$$

where η depends only on a_1 and a_2 , and therefore is a constant independent of frequency. Because η is channel independent, the selected value of η is determined initially by the value of $I(\nu)$, which can be best estimated by the brightness temperature from a selected set of microwave measurements coinciding with the two AIRS FOVs, because microwave measurements in the 50-GHz range are not affected by most types of clouds. The resultant spectral cloud-cleared radiances are then used to retrieve the atmospheric state (temperature and humidity).

In the AIRS cloud-clearing algorithm, we generalize the expansion to 8 degrees of freedom (not all of which are linearly independent), making use of the nine AIRS FOVs within a single AMSU footprints (as illustrated in Fig. 2). This configuration leads to optimal set of coefficients η .

For additional information on the requirements and limitations of this cloud-clearing method we recommend Chahine (1974, 1977) for the basic derivation, and Susskind et al. (2003) for applications to AIRS.

sivity and the solar-reflected component from the (Obs – Calc) evaluation.

In Figs. 4a and 4b we show the results of the analysis for all of the descending (night) orbits of 10 October 2004, restricting our selection to ocean fields within the latitude band extending from 40°S to 40°N. The blue trace is (Obs – Calc) for all accepted cloud-cleared retrievals as determined by Susskind et al. (2006), whereas the red trace is (Obs – Calc) for the reduced subset of the clearest AIRS footprints.

Analysis of the results shown in Figs. 4a and 4b leads to several conclusions. 1) The bias for the clear radiances and the cloud-cleared radiances is the same within 0.2 K. 2) The bias is not zero in specific regions of the spectrum, where the accuracy of the ECMWF

model is in doubt, that is, the region affected by tropospheric water vapor (1500–1600 cm^{-1}) and the region affected by ozone (near 1050 cm^{-1}). 3) Under clear conditions the typical stddev of (Obs – Calc) is about 0.7 K in the tropospheric and surface channels. Because the noise equivalent delta temperature (NeDT) for these channels is typically only 0.2 K, most of this 0.7-K random error in stddev (Obs – Calc) comes from the combination of the computational error if the truth were perfectly known (forward model error) and the error due to discrepancies between ECMWF and the state of the atmosphere observed by AIRS. 4) The 0.7-K stddev (Obs – Calc) in the tropospheric and surface channels under clear conditions increases to 1.1 K for the cloud-cleared radiances. Assuming that errors add

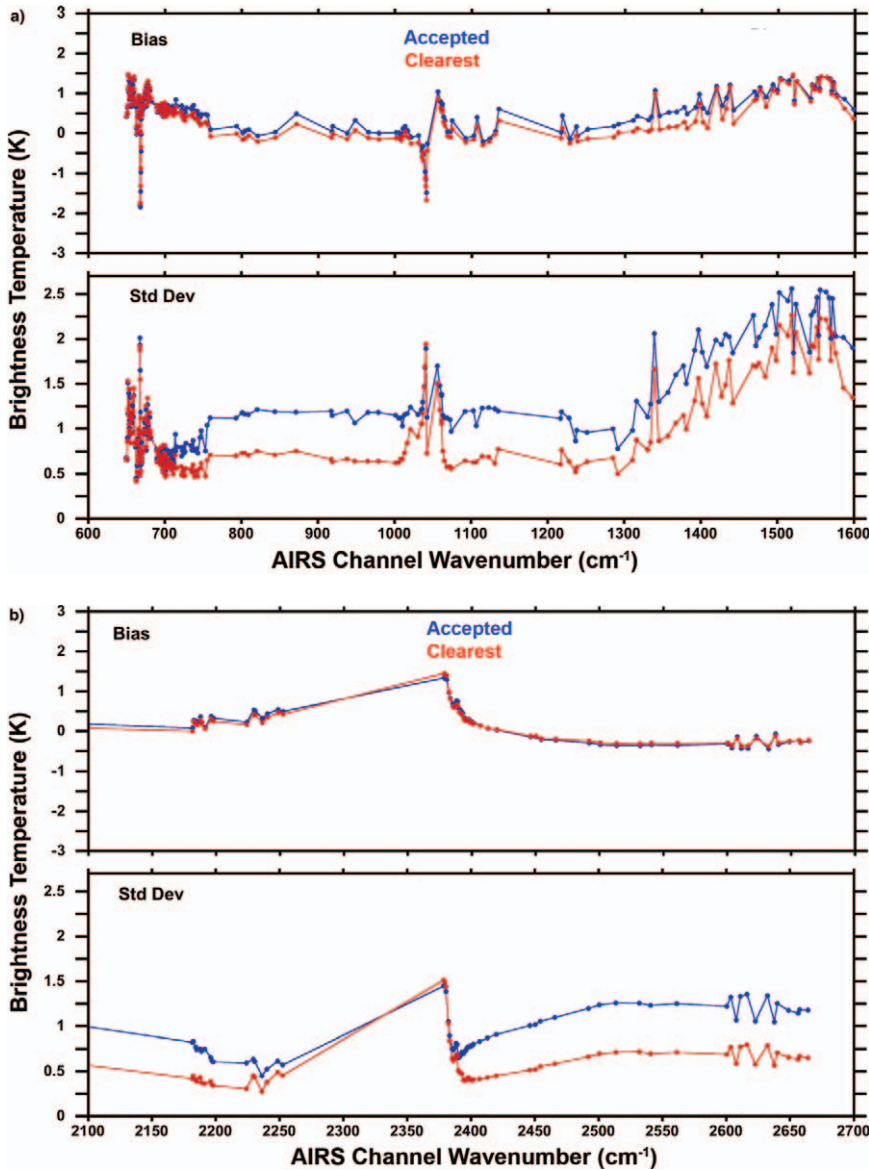


FIG. 4. The (top) bias and (bottom) standard deviation of (Obs - Calc) comparison for the (a) 650–1600 cm^{-1} and (b) 2100–2650 cm^{-1} region. Each dot represents one of the 320 AIRS channels used in the retrieval algorithm.

as the root sum square, cloud clearing therefore added 0.9 K to the noise.

VALIDATION OF TEMPERATURE AND WATER VAPOR PROFILES.² An overview of the AIRS validation activities is provided by Fetzer et al. (2003). The requirement for temperature and moisture soundings from space with radiosonde ac-

curacy has been the driving force for the development of AIRS. An intensive effort of the validation of these soundings showed that global satellite retrievals are in many ways superior to conventional radiosondes, although their vertical resolution cannot quite match that of the point measurements from balloon-borne instruments. The global coverage and high accuracy of temperature and water vapor profiles from space have proven to be a good addition to the traditional radiosondes, particularly over oceans. Satellite retrievals provide a wealth of additional data products not available from conventional radiosondes.

To assess the accuracy of the temperature and the precipitable water vapor profiles retrieved from AIRS, we make use of the validation results obtained at the National Oceanic and Atmospheric Administration (NOAA)/National Environmental Satellite, Data, and Information Service (NESDIS) by Divakarla et al. 2006; hereafter MD) and by Tobin et al. (2006, hereafter DT) of the University of Wisconsin.

The MD study covers several sounders, including AIRS, is global, and makes use of the global operational radiosonde network. The DT validation relies on dedicated radiosondes at two Atmospheric Radiation Measurement (ARM) sites: the Southern Great Plains (SGP) and tropical western Pacific (TWP). Their two validation results are complementary and reveal considerable agreement, which we will discuss in Tables 2 and 3.

² Two versions of the AIRS PRA have been issued so far: version V3 was developed before the launch of *Aqua* and version V4 is an enhanced version currently in use. Each version includes a set of quality checks for the various retrieved parameters, including the retrieved cloud fraction. Version V4 quality checks are strictly internal, and documentation for the versions V3 and V4 is available online at <http://disc.gsfc.nasa.gov/AIRS/documentation/>.

TABLE 2. Components of the near-surface errors (K) in the retrieved temperature profiles. Numbers between parentheses are calculated and numbers without parentheses are carried over or are set equal to zero.

	Rms* error	Clear retrieval	Cloud clearing	Collocation	Emissivity
ARM TWP clearest	0.6	(0.6)	0	0	0
ARM TWP cloud cleared	1.0	0.6	(0.8)	0	0
ARM SGP cloud cleared	2.0	0.6	0.8	0	(1.7)
Global ocean clearest	1.0	0.6	0	(0.8)	0
Global ocean cloud cleared	1.4	0.6	(1.0)	0.8	0
Global land cloud cleared	1.7	0.6	1.0	0.8	(0.9)

* From retrieval validation results.

TABLE 3. Components of the near-surface percent errors in the retrieved precipitable water vapor profiles. Numbers between parentheses are calculated and numbers without parentheses are carried over or are set equal to zero.

	RMS* error	Clear retrieval/ cloud clearing**	Collocation	Emissivity
ARM TWP clearest	10%	(10%)	0	0
ARM TWP cloud cleared	10%	10%	0	0
ARM SGP cloud cleared	25%	10%	0	(23%)
Global ocean clearest	17%	10%	(14%)	0
Global ocean cloud cleared	16%	10%	14%	0
Global land cloud cleared	25%	10%	14%	(18%)

* From retrieval validation results.

** We cannot separate the contributions of the retrieval and cloud-clearing errors due to nonnegligible uncertainty in the first column rms error.

Divakarla collected approximately 10^5 matchups from September 2002 to December 2004, mostly from the Northern Hemisphere. For a matchup to be accepted the radiosonde measurement must be within ± 3 h and 100 km from the AIRS overpass. The AIRS-retrieved profiles were derived using version V4 of the PRA. Applying the version V4 quality checks reduced the dataset of matchups to 59,433 (60% yield). This number includes a subset of the 999 “clearest” matchups. The resultant dataset contained an equal number of day and night cases. However, due to the scarcity of oceanic radiosonde stations, only 5,330 cases corresponded to oceans while 17,799 corresponded to land. The remainder were coastal areas, in which both land and ocean are present in an AIRS retrieval footprint. The zonal distribution

of these data is as follows: 8% tropical (23°N – 23°S), 44%, midlatitude (50° – 23°N and 50° – 23°S), and 48% high latitude (90° – 50°N and 90° – 50°S). Only 420 of the ocean cases were classified as clearest retrievals and there were none over land. Figure 5 shows the rms differences of a 1-km-layer mean temperature profiles for clear (red), and cloud-cleared oceans (blue), and land (green). The rms differences are largest near the surface. Figure 6 shows the rms percent difference of 2-km-layer integrated precipitable water vapor profiles according to MD.

Similar rms differences (not shown in this paper) were obtained by DT, who minimized the temporal and collocation mismatch between radiosondes and AIRS overpasses by using well-timed, dedicated radiosondes. The DT dataset contained a total of

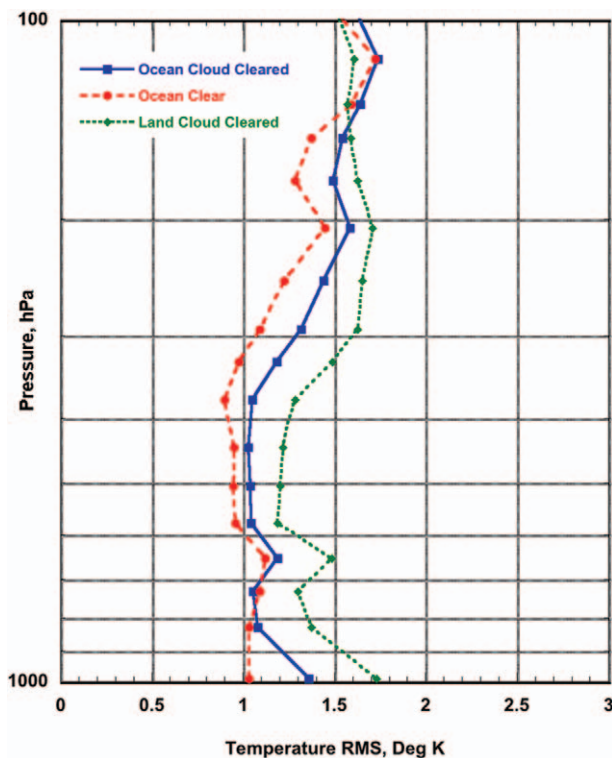


FIG. 5. Global comparison of AIRS temperature profiles with radiosondes for ocean clear, ocean cloud-cleared, and land cloud-cleared conditions.

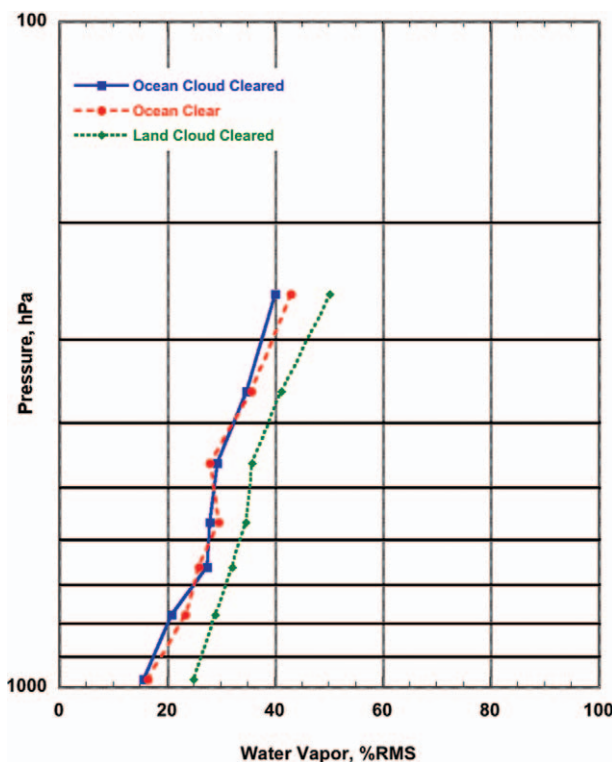


FIG. 6. Global percent errors of AIRS precipitable water vapor profiles with respect to radiosondes for ocean clear, oceans cloud-cleared, and land cloud-cleared conditions.

79 overpasses at the tropical equatorial ocean TWP site and 151 for the midlatitude land SGP site. Of these, 55% passed the AIRS version V4 quality check, including 10% classified as being the clearest retrievals.

Closer comparison between the results from MD and DT shows a distinct pattern: as the scene complexity increases from clear ocean to cloudy land the rms difference between the estimated true state of the atmosphere and that retrieved from the AIRS data increases. This suggests that the observed rms difference can be expressed as the combination of a number of components. To estimate the contribution of each component we use the expression

$$(\text{Observed})_{\text{RMS}}^2 = (\text{Clear Retrieval})_{\text{RMS}}^2 + (\text{Cloud - Cleared})_{\text{RMS}}^2 + (\text{Collocated})_{\text{RMS}}^2 + (\text{Emissivity})_{\text{RMS}}^2$$

which states that the square of the observed rms difference between the estimated true state of the atmosphere and that retrieved by AIRS is the sum of four terms: 1) the retrieval accuracy under perfectly cloud-free and uniform scene conditions (this term includes the effects of Gaussian random instrument noise, the forward model error, the error due to uncertainty in the column abundances of CO_2 , currently fixed at 370 ppmv, and “computational noise” from approximations used in other steps of the retrieval process as discussed in Susskind et al. 2003), 2) the error introduced by the process to eliminate the effects of clouds, 3) the error introduced by uncertainties in the surface emissivity, and 4) the temporal and spatial collocation error, that is, the difference between the state of the atmosphere observed from space in a 45-km beam of the AMSU field of view (FOV) and the ascent-path observations by radiosondes launched up to 100 km and 3 h from the satellite overpass. We assumed the radiosondes to be the “truth.” No radiosonde errors are considered.

In Tables 2 and 3, the first column is taken from the results of DT and MD. We chose the region within 1–2 km above the surface, where the errors are largest, because it is strongly affected by all four of the above terms. For the TWP clearest subset (first row), all of the terms on the right-hand side of the above equation are negligible, except for the retrieval errors, which are equal to 0.6 K. For the cloud-cleared case (second row) we assume the retrieval error is unchanged and compute the cloud-clearing error as 0.8 K. Similarly for the SGP site (third row), we carry the clear retrieval and cloud-clearing errors

(third row) and compute the surface emissivity error to be 1.7 K, noting that DT's dataset has negligible collocation error. Next, we apply the same steps to the global dataset, and assuming the same retrieval error we compute for the clear cases a collocation error of 0.8 K and a cloud-clearing error of 1.0 K. Table 3 is similar to Table 2 except that the analysis is done for the lower-tropospheric precipitable water vapor.

The results from Tables 2 and 3 are revealing. We note the similarities between the two validation datasets. For the clearest fraction a retrieval accuracy of 0.6-K rms for temperature and 10% for water near the surface are achieved. For the 55% cloud-cleared retrievals, AIRS achieves about 1-K rms accuracy over ocean, and about 1.7 K over land. In general, we found that cloud-clearing error dominates over the ocean and the surface emissivity error dominates over land. The 55% yield and the 1-K rms-estimated cloud-clearing error for this dataset is consistent with the 50% yield and 0.9-K rms cloud-clearing error deduced from the (Obs - Calc) evaluation in the previous section.

Typically, we combine many retrieved profiles like those shown in Figs. 5 and 6 to create global AIRS level 3 (L3) data products, such as the total precipitable water vapor given in Fig. 7. The upper panel shows the upper-troposphere total water vapor above the 500-hPa level and the lower panel shows the total precipitable water for the entire atmosphere, for the month of January 2003. Upper-tropospheric water vapor monthly maps like these, as well as 1-day and 8-day compilations, are easily generated from the standard AIRS data product and are available at the NASA Goddard Space Flight Center (GSFC) Distributed Active Archive Center (DAAC).

The accuracy of the integrated water vapor in Fig. 7 has been cross compared with the Advanced Microwave Sounder-EOS (AMSRE), a companion instrument on *Aqua* (see Fetzer et al. 2006).

AIRS DATA ASSIMILATION FOR NWP. *On the learning curve.* Several NWP centers around the world are currently receiving subsets of AIRS radiance data through NOAA/NESDIS (Goldberg et al. 2003). These centers include NCEP, NASA, NOAA, Department of Defense (DoD) Joint Center for Satellite Data Assimilation (JCSDA), the Canadian Meteorological Centre (CMC), Japan Meteorological Agency (JMA), the Fleet Numerical Meteorology and Oceanography Center (FNMOC), the Met Office (UKMO), ECMWF, and Météo France. Although less than 1% of the AIRS spectra are currently selected

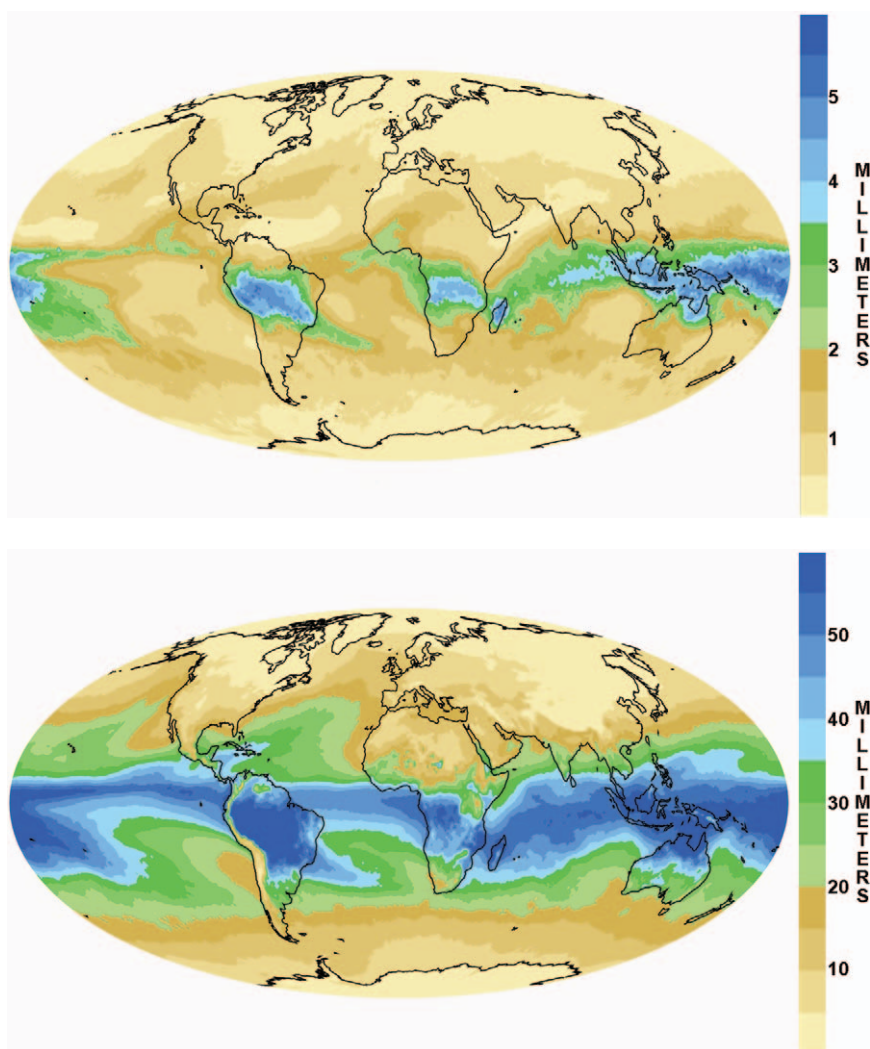


FIG. 7. (top) AIRS precipitable water vapor from 500 hPa to the top of the atmosphere for January 2003. (bottom) AIRS total precipitable water vapor for January 2003.

to be used for data assimilation, the results are encouraging. The task of incorporating the full AIRS radiance data product is still ongoing. Adjusting to the assimilation of the much larger amount of data is a learning process that takes time. At present, three of these centers, ECMWF, NCEP, and the UKMO, have been assimilating AIRS data in their operational forecasts. All have reported positive impacts due to AIRS radiance assimilation.

Radiance assimilation. AIRS radiance data have been assimilated in trials using the operational NCEP Global Forecast system (GFS) at the NASA, NOAA, and DoD Joint Center for Satellite Data Assimilation. The goal was to assess the impact of AIRS data on an operational global forecast system in both the Northern and Southern Hemispheres. Results for January 2004 are reported by Le Marshall et al. (2005a,b, also the companion paper in *BAMS*, Le Marshall et al. 2006). Consistent results have been obtained for August–September 2004 (Le Marshall et al. 2005c). The impact for January is displayed in Figs. 8a and 8b, where the anomaly correlations were calculated for forecasts from 1 to 27 January 2004 with and without inclusion of AIRS radiance observations. The benefit to the GFS, which had also

assimilated the full operational database, is clear. The several-hour increase in forecast range at 5–6 days usually takes several years to achieve at operational weather forecast centers. The magnitude of the increase reported in these studies, particularly in the Northern Hemisphere, has been shown to be related to the use of the full spatial resolution AIRS database, rather than the use of the subset of 1 in 18 or 1 in 9 fields of view usually employed for operational NWP application of the data. JCSDA forecast also benefits from the use of 250 channels of data. The operational use of these AIRS data at NCEP followed the June 2005 operational upgrade.

Assimilation of retrieved parameters. In parallel with the assimilation of radiances by JCSDA, Atlas (2005) at NASA’s GSFC has been assimilating the less voluminous set of retrieved level 2 temperature profiles, using version V3 of the retrieval algorithm. He has shown forecast impact, particularly in the Southern Hemisphere, and an improvement in forecasting the intensity and position of cyclones. The initial experiments at GSFC were conducted using the so-called FVSSI data assimilation system, which represents the combination of the NASA finite-volume general circulation model (FVGCM) with NOAA/NCEP spectral statistical interpolation (SSI) analysis. For the month of January 2003, a control was generated in which the full operational database [including all conventional data, QuikSCAT, Special Sensor Microwave Imager (SSM/I), atmospheric motion winds, and ATOVS radiances from NOAA-14, -15, and -16] was assimilated, and 5-day global forecasts were then generated every 24 h. This was followed by a corresponding assimilation and forecasts that added AIRS clearest and partially cloudy temperature retrievals to the control. In this experiment, AIRS temperatures profiles were assimilated over oceans only and were thinned to a resolution of 100 km.

Figures 9a and 9b summarize the impact of version V3 retrievals of temperature on 5-day forecasts using the FVSSI. In Fig 9a for the Southern Hemisphere, there is a significant positive impact from days 3 to 5 when all of the AIRS data are assimilated. When only the clearest AIRS retrievals are assimilated, the impact is only very slightly positive on average. In the Northern Hemisphere (Fig. 9b), there is a slight positive impact when both clear and partially cloudy data are assimilated, and a slight negative impact when only clear AIRS data are assimilated. These results, in agreement with the previous Observing System Simulation Experiments (OSSEs) for AIRS,

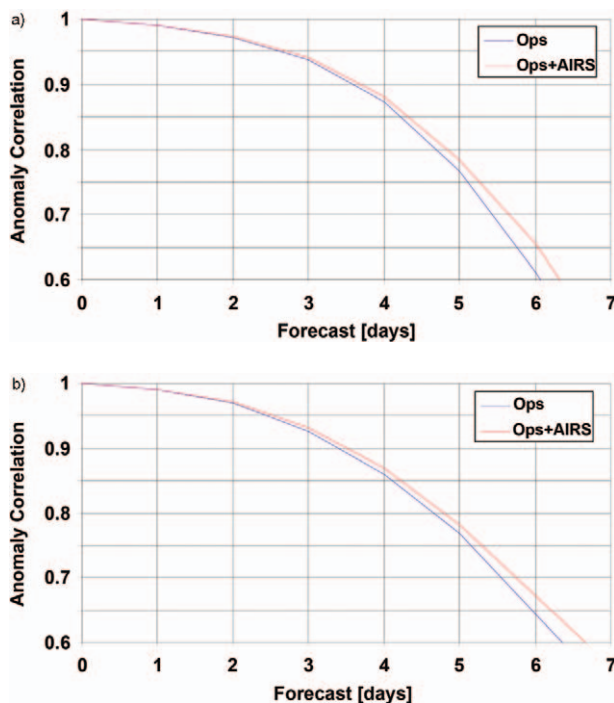


FIG. 8. January 2004 forecast anomaly correlations for the Operational GFS (Ops) and the Operational GFS augmented with AIRS data (Ops+AIRS) for the (a) Southern Hemisphere and (b) Northern Hemisphere (JCSDA).

demonstrate the importance of effective cloud clearing and the need to assimilate partially cloudy data. Nevertheless, these results are from initial experiments (on the learning curve), and it is possible to improve the assimilation of clear AIRS retrievals beyond the results reported here.

The anomaly correlations shown in Figs. 9a and 9b represent an average of positive and negative impacts over many cases. In the Northern Hemisphere, 12 of the 26 forecast cases of this particular experiment were positive impacts, while 5 were negative. In the Southern Hemisphere, 16 cases were positive impacts, while 6 were negative. Figures 10a and 10b present representative examples of the types of improvement that can occur in each hemisphere.

As an illustration of the level of improvement in the Northern Hemisphere, Fig. 10a shows the impact of AIRS physical retrievals on the 5-day prediction of an extratropical cyclone and trough in the North Atlantic. AIRS data give a significant forecast improvement over the control for this experiment, as measured by the locations of both the cyclone and the trough to its south.

Figure 10b shows another illustration of significant impact of AIRS retrievals on an extratropical cyclone in the South Pacific. The 96-h control forecast (shown in the upper-left panel) fails to predict the intense (950 hPa) cyclone located at 64°S, 150°W, and instead predicts a spurious, weaker cyclone far to the northwest of the observed location. In contrast the 96-h forecast that included AIRS retrievals (shown in the upper-right panel) provides a very accurate prediction of both the location of the storm and its intensity.

The Goddard Laboratory for Atmospheres and the Joint Center for Satellite Data Assimilation are continuing to perform forecast studies with AIRS data, and will compare results of the assimilation of radiances with the assimilation of newer versions of the AIRS retrievals (versions V4 and beyond).

ATMOSPHERIC COMPOSITION—MINOR GASES. AIRS radiances are sensitive to variations in airborne particulate matter and the concentration of several minor gases. Retrieval algorithms have been developed to produce important “research data products” including aerosol optical thickness and concentrations of minor gases, including O₃, sulfur dioxide (SO₂), CH₄, CO, and CO₂. A sample of current retrievals of atmospheric minor constituents is presented in this section. After validation, these products will be retrieved routinely as part of an updated AIRS retrieval algorithm.

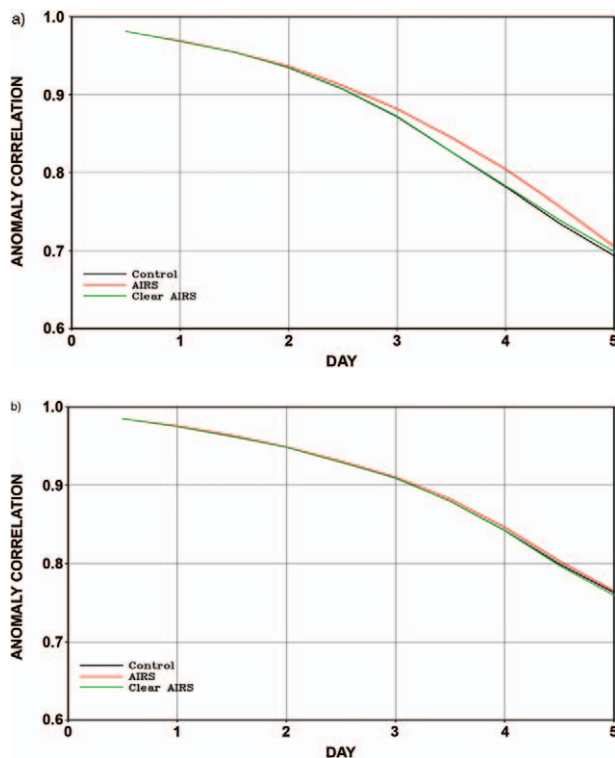
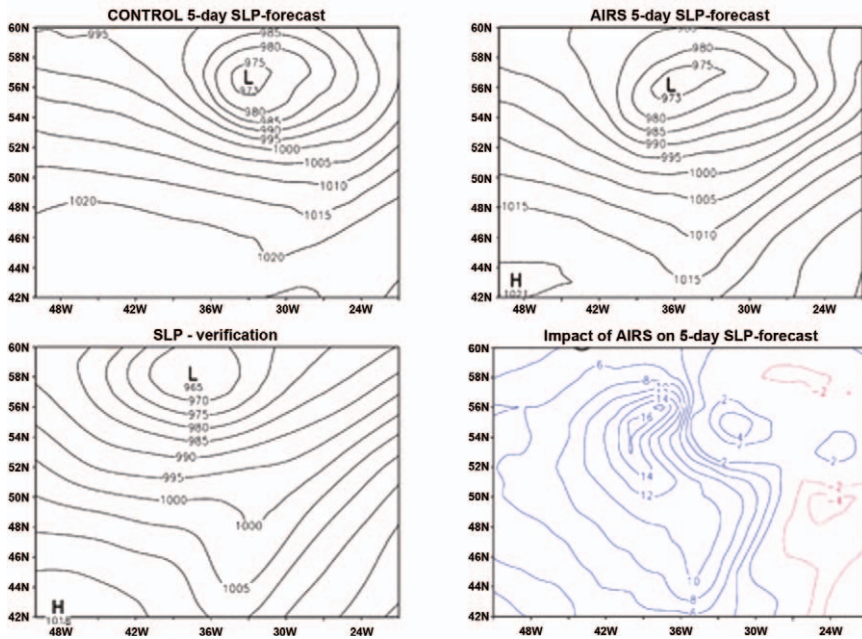


FIG. 9. Accuracy of the control AIRS (control plus clearest and partially cloudy AIRS data), and clearest AIRS (control plus clearest AIRS data) 5-day forecasts for the (a) Southern Hemisphere and (b) Northern Hemisphere in January 2003.

Carbon dioxide. In the 712–750 cm⁻¹ region, CO₂ is one of the most important minor gases retrieved from AIRS spectral radiances. The AIRS CO₂ retrieval uses an analytical method based on the properties of partial derivatives for the determination of carbon dioxide and other minor gases in the troposphere from AIRS spectra. Chahine et al. (2005) applied this method to derive the mixing ratio of carbon dioxide and compared the AIRS results to aircraft flask measurements of carbon dioxide made by Matsueda et al. (2002). The results of AIRS CO₂ retrieval demonstrated skill in tracking the flask-measured seasonal variation with an accuracy of 0.43 ± 1.20 ppmv.

Carbon monoxide. Tropospheric carbon monoxide (CO) abundance is retrieved from the 2180–2230 cm⁻¹ region of the IR spectrum. Given that CO is the direct product from the combustion of fossil fuel and biomass burning, and that it has a role as a smog and tropospheric ozone precursor, finescale global observations of CO are crucial for modeling tropospheric chemistry and assessing the impact of biomass burning on the atmosphere. Using the AIRS 1600-km

a) IMPACT OF AIRS ON 5-DAY FORECAST OF A CYCLONE AND TROUGH IN THE NORTH ATLANTIC FORECAST VERIFIED AT 00 UTC / 16 JANUARY 2003



b) IMPACT OF AIRS ON A 96-HOUR FORECAST VERIFIED AT 00 UTC / 18 JANUARY 2003

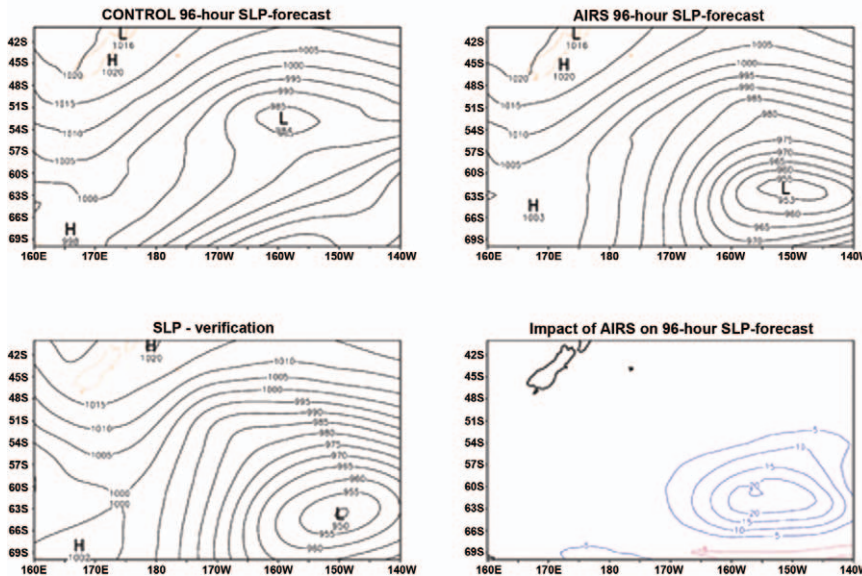


FIG. 10. (a) Sea level pressure for the North Atlantic: (top left) 5-day control forecast, (top right) 5-day control + AIRS forecast, (bottom left) verifying analysis, (bottom right) impact of AIRS, where blue contours represent improvement (GSFC). Forecast verified at 0000 UTC 16 Jan 2003. (b) Assimilation of AIRS retrievals using the FVSSI has resulted in a very significant improvement in the position and intensity of an intense cyclone in the South Pacific (GSFC). 96-h forecast verified at 0000 UTC 18 Jan 2003.

cross-track swath and cloud-clearing retrieval capabilities, retrieved daily global CO maps cover approximately 70% of the Earth, as shown in Fig. 11 for the week of 22–29 September 2002. Extremely

of the Northern (summer) Hemisphere. This difference may be due to interference by dust and aerosol from biomass burning, and errors in emissivity over land areas. However, it *may* be possible that AIRS

high CO concentration can be seen as a result of biomass burning over central South America, Africa, and Indonesia with evidence for significant transport to the South Atlantic and Indian Oceans. Preliminary validation by McMillan et al. (2005) indicates that AIRS CO retrievals are approaching the 15% accuracy in column amount target set by prelaunch simulations.

Ozone. AIRS radiance data in the 9.6- μm band are used to retrieve column ozone and ozone profiles for both day and night (including the polar night). Figure 12 shows the mean total ozone for January 2003, while Fig. 13 compares version 4 AIRS total column ozone with version 8 gridded results from the Total Ozone Mapping Spectrometer (McPeters et al. 1998) for 6 September 2002. TOMS relies on backscattered ultraviolet radiation to measure total ozone. Only AIRS retrievals that were successful at every processing step are compared. Between 50°S and 50°N, AIRS total column ozone is on average higher than TOMS by 1.3 ± 6.4 DU (1σ). AIRS tends to be lower than TOMS in the tropical western Pacific, and preliminary evaluations suggest that this difference is related to interference from high, cold cirrus clouds. AIRS also tends to be higher than TOMS throughout much

legitimately yields higher column amounts than TOMS in some regions because of scattering of the TOMS signal in the lower troposphere (see Martin et al. 2002, and references therein). Work to quantify and validate AIRS sensitivity to tropospheric ozone is currently underway.

Aerosols. AIRS can detect the infrared signature of aerosols in the atmosphere. Silicate aerosols feature peaks in the 900–1100 cm^{-1} region, while both ice and aerosols show minimal absorption around at 1232 cm^{-1} . Figure 14 shows the brightness temperature difference between AIRS radiances at 961 and 1232 cm^{-1} (DeSouza-Machado et al. 2006). Aerosol features currently affect the accuracy of temperature and water vapor retrievals, but it is believed that a variant of this aerosol detection algorithm can be used as a quality control measure or as a means to correct for the aerosol effects in the meteorological retrieval process. Note that Fig. 14 shows the monthly mean of the aerosol distribution, with the color-scale lower limit truncated above the maximum negative signal coming from west of Africa to highlight smaller dust features.

Sulfur dioxide. AIRS spectra have been used to observe the total column of SO_2 injected into the atmosphere during a volcanic event. Figure 15 (left) is the image derived from AIRS visible

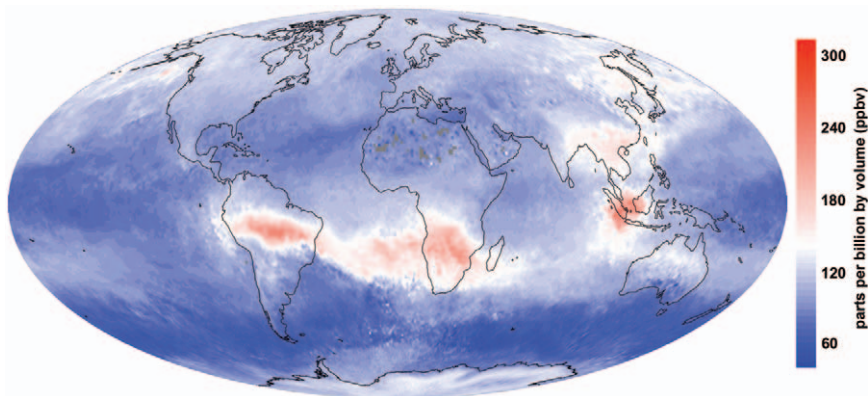


FIG. 11. AIRS CO for 22–29 Sep 2002; high CO concentration results are from biomass burning in South America, Africa, and Indonesia.

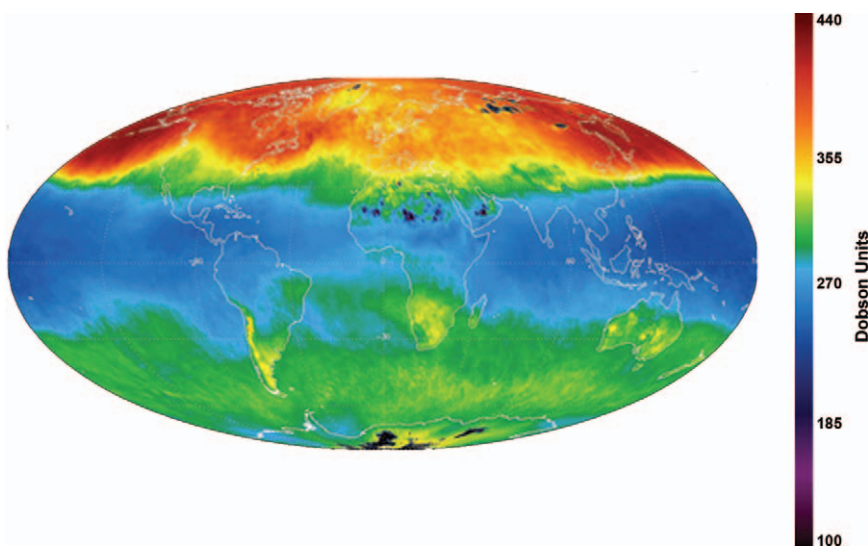


FIG. 12. Global distribution of total ozone for the month of January 2003.

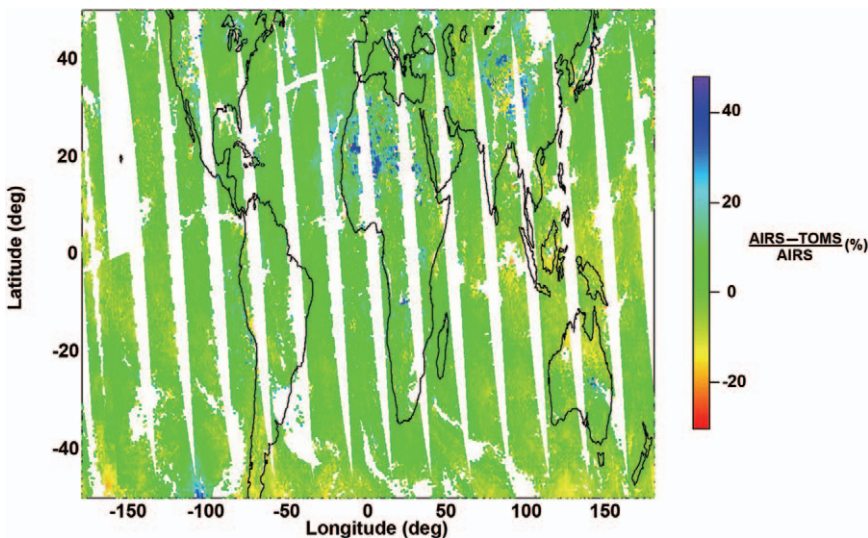


FIG. 13. Difference between version V4 AIRS and V8 TOMS total ozone measurements for 6 Sep 2002. No AIRS retrievals are obtained in white areas.

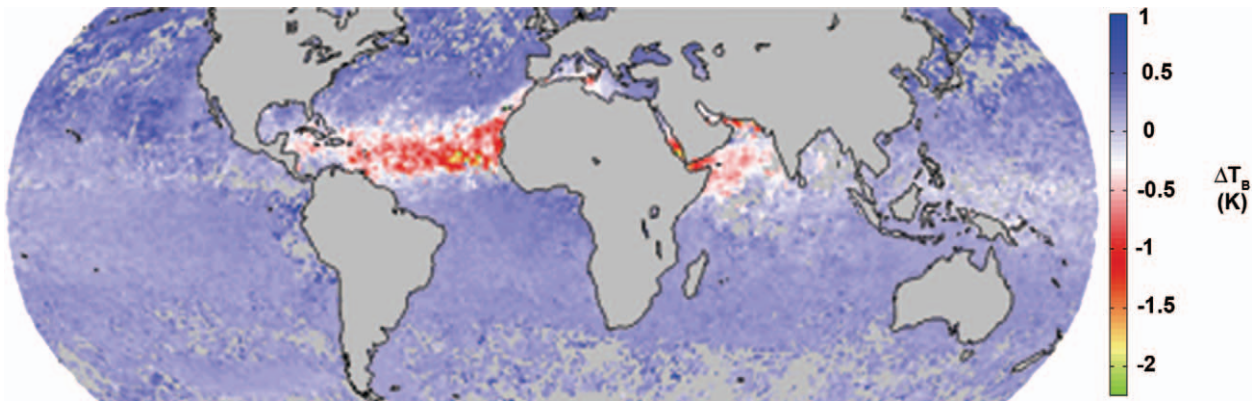


FIG. 14. Global aerosol retrieved (shown in terms of brightness temperature difference) for the month of July 2003. The dust storm from Africa is transported across the Atlantic all the way to Central America.

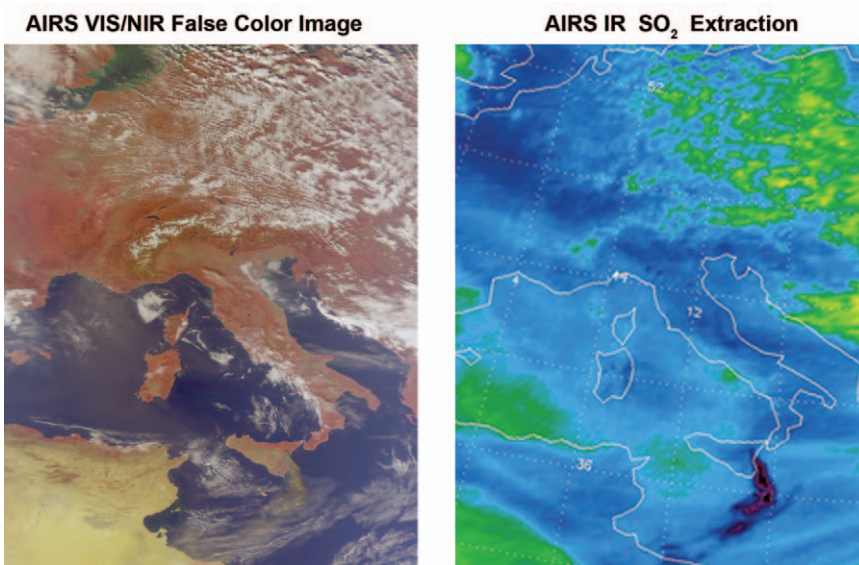


FIG. 15. AIRS (left) visible image and (right) SO_2 of the 2002 Mt. Etna eruption using a simple IR channel differencing approach.

channels, showing a plume from the volcanic eruption of Mt. Etna in Italy on 28 October 2002. Figure 15 (right) also shows the result of a simple two-channel extraction of the SO_2 signature. AIRS channels at 1258.90 and at 1354.10 cm^{-1} were used in the analysis (Carn et al. 2005). Both channels are sensitive to water vapor, but one of the channels is also sensitive to SO_2 . By subtracting out the common water vapor signal in both channels, the SO_2 feature remains as a clear feature in the difference image.

SUMMARY AND CONCLUSIONS. The AIRS instrument has met its primary scientific objective to improve weather prediction and to retrieve temperature and precipitable water vapor profiles with accuracies approaching those of radiosondes. AIRS also has provided new information on the concen-

tration of tropospheric minor constituents, including several greenhouse gases essential for climate studies.

The foundation of all AIRS data products is the physical retrieval algorithm (PRA) that is being maintained and continuously upgraded by the AIRS Science Team. The results described in this paper are “work in progress,” and although significant accomplishments have already been made, much more work remains in order to realize the full potential of this instrument. The AIRS

Science Team is currently pursuing improvements to the retrieval algorithm, in particular 1) determination of land surface emissivity, 2) modification of the radiative transfer algorithm (RTA) to account for nonlocal thermodynamic equilibrium (NLTE) effects on the shortwave channels, 3) development of a cloud-clearing algorithm based on AIRS spectra only, and 4) incorporation of variable atmospheric CO_2 in the RTA. In addition, the team is developing plans for validation of the AIRS-retrieved minor constituents, and further validation of the water vapor profiles in the upper troposphere remains a very high priority.

Information on AIRS progress, publications, and other educational materials can be accessed from the AIRS Web site at <http://airs.jpl.nasa.gov>. Additionally, the GSFC DAAC has an extensive library of AIRS data that can be accessed at their Web site at <http://daac>.

gfs.nasa.gov. Also available on this Web site is user guide information that describes the contents of the files, how to read the hierarchical data format, and the validation reports discussing the quality of the level 1 and level 2 products.

While discussions here are focused on AIRS on *Aqua*, it is clear that the knowledge and experience gained from AIRS will also benefit future satellite programs based on infrared radiance measurements, such as the Cross-track Infrared Sounder (CrIS) on the National Polar-orbiting Operational Environmental Satellite System (NPOESS), the Infrared Atmospheric Sounding Interferometer (IASI) on the European Meteorological Satellite (EUMETSAT) Meteorological Operational (METOP) series, and the Hyperspectral Environmental Suite (HES) for the Geostationary Operational Environmental Satellites (GOES)-R.

ACKNOWLEDGMENTS. We wish to thank Fred G. O'Callaghan, the first AIRS Project Manager, for his meticulous care in the design, building, and testing of the AIRS instrument. We wish also to acknowledge Paul Morse and the dedicated team of engineers and managers at BAE SYSTEMS for building a near-perfect sounder. The AIRS project was initiated under Dr. Shelby Tilford, NASA Associate Administrator for Earth Science. His vision and leadership were essential for the accomplishment of this work.

This work was carried out in parts at the Jet Propulsion Laboratory, California Institute of Technology, under contract with the National Aeronautics and Space Administration.

REFERENCES

- Atlas, R., 2005: The impact of AIRS data on weather prediction. *Proc. SPIE Conf. Algorithms Technol. Multispectral Hyperspectral Ultraspectral Imagery XI*, **5806**, 599–606.
- Aumann, H. H., and Coauthors, 2003a: AIRS/AMSU/HSB on the *Aqua* mission: Design, science objectives, data products, and processing systems. *IEEE Trans. Geosci. Remote Sens.*, **41**, 253–264.
- , —, and D. Barron, 2003b: Sea surface temperature measurements with AIRS: RTG.SST comparison. *Proc. SPIE*, **5151**, 252–260.
- , D. Gregorich, and D. Barron, 2004: Spectral cloud-filtering of AIRS data: Non-polar ocean. *Proc. SPIE*, **5548**, 313–320.
- , S. Broberg, D. Elliot, S. Gaiser, and D. Gregorich, 2006: Three years of AIRS radiometric calibration validation using sea surface temperatures. *J. Geophys. Res.*, **111**, doi:10.1029/2005JD006822.
- Carn, S. A., L. L. Strow, S. G. de Souza-Machado, Y. Edmonds, and S. E. Hannon, 2005: Quantifying tropospheric volcanic emissions with AIRS: The 2002 eruption of Mt. Etna (Italy). *Geophys. Res. Lett.*, **32**, L02391, doi:10.1029/2004GL021034.
- Chahine, M. T., 1974: Remote sounding of cloudy atmospheres. I. The single cloud layer. *J. Atmos. Sci.*, **31**, 233–243.
- , 1977: Remote sensing of cloudy atmospheres II: Multiple cloud formations. *J. Atmos. Sci.*, **34**, 744–755.
- , 1981: Remote sensing of sea-surface temperature in the 3.7 μm CO₂ band. *Oceanography from Space*, J. F. R. Gower, Ed., Plenum Press, 87–95.
- , 1992: The hydrological cycle and its influence on climate. *Nature*, **359**, 373–380.
- , and Coauthors, cited 2001: AIRS level 2 unified retrieval for core products ATBD. [Available online at http://eospsso.gsfc.nasa.gov/eos_homepage/for_scientists/atbd/].
- , C. Barnet, E. T. Olsen, L. Chen, and E. Maddy, 2005: On the determination of atmospheric minor gases by the method of vanishing partial derivatives with application to CO₂. *Geophys. Res. Lett.*, **32**, L22803, doi:10.1029/2005G1024165.
- DeSouza-Machado, S. G., L. L. Strow, S. E. Hannon, and H. E. Motteler, 2006: Infrared dust spectral signatures from AIRS. *Geophys. Res. Lett.*, **33**, L038, doi:10.1029/2005GL024364.
- Divakarla, M., G. C. D. Barnet, M. D. Goldberg, L. M. McMillin, E. Maddy, W. Wolf, L. Zhou, and X. Liu, 2006: Validation of Atmospheric Infrared Sounder temperature and water vapor retrievals with matched radiosonde measurements and forecasts. *J. Geophys. Res.*, **111**, D09S15, doi:10.1029/2005JD006116.
- Fetzer, E., and Coauthors, 2003: AIRS/AMSU/HSB validation. *IEEE Trans. Geosci. Remote Sens.*, **41**, 418–431.
- , B. Lambrigtsen, A. Eldering, H. H. Aumann, and M. T. Chahine, 2006: Biases in total precipitable water vapor climatologies from Atmospheric Infrared Sounder and Advanced Microwave Scanning Radiometer. *J. Geophys. Res.*, **111**, D09S16, doi:10.1029/2005JD006598.
- Goldberg, M. D., Y. Qu, L. M. McMillin, W. Wolf, L. Zhou, and M. Divakarla, 2003: AIRS near-real-time products and algorithms in support of operational numerical weather prediction. *IEEE Trans. Geosci. Remote Sens.*, **41**, 379–389.
- Houghton, J. T., Y. Ding, D. J. Griggs, M. Noguer, P. J. van der Linden, X. Dai, K. Maskell, and C. A. Johnson, Eds., 2001: *Climate Change 2001: The Scientific Basis*. Cambridge University Press, 944 pp.

- Le Marshall, and Coauthors, 2005a: AIRS hyperspectral data improves southern hemisphere forecasts. *Aust. Meteor. Mag.*, **54**, 57–60.
- , and Coauthors, 2005b: Impact of Atmospheric InfraRed Sounder observations on weather forecasts. *EOS, Trans. Amer. Geophys. Union*, **86**, 109, 115, 116.
- , and Coauthors, 2005c: AIRS associated accomplishments at the JCSDA—First use of full spatial resolution hyperspectral data show significant improvements in global forecasts. *Proc. SPIE*, **5890**, doi:10.1117/12.6157-57.
- , and Coauthors, 2006: Advanced InfaRed Sounder (AIRS) observations improve global analysis and forecast capability. *Bull. Amer. Meteor. Soc.*, in press.
- Martin, R. V., and Coauthors, 2002: Interpretation of TOMS observations of tropical tropospheric ozone with a global model and in situ observations. *J. Geophys. Res.*, **107**, 4351, doi:10.1029/2001JD001480.
- Matsueda, H., H. Y. Inoue, and M. Ishii, 2002: Aircraft observation of carbon dioxide at 8–13 km altitude over the western Pacific from 1993 to 1999. *Tellus*, **54B**, 1–21.
- McMillan, W. W., and Coauthors, 2005: Daily global maps of carbon monoxide from NASA's Atmospheric Infrared Sounder. *Geophys. Res. Lett.*, **32**, L11801, doi:10.1029/2004GL021821.
- McPeters, R. D., and Coauthors, 1998: Earth probe Total Ozone Mapping Spectrometer (TOMS) data products user's guide. NASA Reference Publication 206895, 69 pp.
- National Research Council, 2004: *Implementing Climate and Global Change Research: A Review of the Final US Climate Science Change Program*. National Academies Press, 108 pp.
- Pagano, T. S., H. H. Aumann, D. Hagan, and K. Overoye, 2003: Pre-launch and in-flight radiometric calibration of the Atmospheric Infrared Sounder (AIRS). *IEEE Trans. Geosci. Remote Sens.*, **41**, 266–273.
- Strow, L. L., S. E. Hannon, S. De-Souza Machado, H. E., Motteler, and D. C. Tobin, 2006: Validation of the Atmospheric Infrared Sounder radiative transfer algorithm. *J. Geophys. Res.*, **111**, D09S06, doi:10.1029/2005JD006146.
- Susskind, J., C. Barnet, and J. Blaisdell, 2003: Retrieval of atmospheric and surface parameters from AIRS/AMSU/HSB data in the presence of clouds. *IEEE Trans. Geosci. Remote Sens.*, **41**, 390–409.
- , —, —, L. Iredell, F. Keita, L. Kouvaris, G. Molnar, and M. Chahine, 2006: Accuracy of geophysical parameters derived from AIRS/AMSU as a function of fractional cloud cover. *J. Geophys. Res.*, **111**, D09S17, doi:10.1029/2005JD006272.
- Tian, B., D. E. Waliser, E. Fetzer, B. Lambriksen, Y. Yung, and B. Wang, 2006: Vertical moist thermodynamic structure and spatial–temporal evolution of the Madden–Julian oscillation in AIRS observations. *J. Atmos. Sci.*, in press.
- Tobin, D., and Coauthors, 2004: Validation of Atmospheric Infrared Sounder (AIRS) spectral radiances with the Scanning High-resolution Interferometer Sounder (S-HIS) aircraft instrument. *SPIE*, **5571**, 383–392.
- , and Coauthors, 2006: Atmospheric Radiation Measurement site atmospheric state best estimates for AIRS temperature and water vapor retrieval validation. *J. Geophys. Res.*, **111**, D09S14, doi:10.1029/2005JD006103.
- Walden, V., W. Roth, R. S. Stone, and B. Halter, 2006: Radiometric validation of the Atmospheric Infrared Sounder (AIRS) over the Antarctic Plateau. *J. Geophys. Res.*, D09S03, doi:10.1029/2005JD006357.